Remote Sensing of Environment 113 (2009) 2258–2266

Contents lists available at ScienceDirect

Remote Sensing of Environment

journal homepage: www.elsevier.com/locate/rse

Spatial and temporal dynamics of river channel migration and vegetation in central Amazonian white-water floodplains by remote-sensing techniques

Juliana Maerschner Aguiar Peixoto [a], Bruce Walker Nelson [a], Florian Wittmann [b,*]

[a] Instituto Nacional de Pesquisas da Amazônia, Av. André Araújo 2936, 69060-001 Manaus, Brazil
[b] Max Planck Institute for Chemistry, Biogeochemistry Department, Johann J Becher-Weg 27, 52180 Mainz, Germany

ARTICLE INFO

Article history:
Received 9 October 2008
Received in revised form 19 June 2009
Accepted 20 June 2009

Keywords:
Alluvial geomorphology
Cecropia forest
Central Amazon basin
C-sequestration
Remote sensing
Várzea
Vegetation
Wetland mapping

ABSTRACT

We investigated spatial and temporal migration of the Solimões, the Japurá, and the Aranapu River channels in western Brazilian Amazonia with Landsat TM imagery over a 21-year period. Additionally, we classified and monitored how channel migrations affect the distribution of pioneer vegetation and old-growth forest. The cloud-free study area was 153,032 ha — open water plus 3 km inland on each margin. The channel migration rates, expressed as percent dislocation of the open water body of the river year^{-1}, were lowest in the Japurá River (1.2%), and highest in the Aranapu channel (2.5%), the point bars at river confluence being the most affected landforms subject to geomorphic changes. Annual rates of lateral erosion and accretion of vegetated land along the three rivers were well-balanced. They averaged 0.79 and 0.83% of the cloud-free channel area over the 21 years. The Solimões River was more dynamic than the Japurá River, which can be traced to higher water discharge and sediment load. During the 21 years, the area covered by pioneer vegetation increased by 5.8% of the study area, while late-succession areas decreased by a similar amount (5.5%). According to local biomass estimates of the different vegetation types, these values suggest that C-releases by alluvial erosion would be much higher than C-sequestration caused by the creation of areas suitable for colonization by pioneer vegetation at our study site.

1. Introduction

Amazonian white-water rivers originate from the Andes or the Sub-Andean foothills, and they carry large suspended sediment loads, deposited in lowlands further east. With a water discharge of 70,000–130,000 m^3 s^{-1}, the Ucayali–Solimões–Amazon River is the largest Amazonian white-water river. Above its confluence with the Negro River in central Brazilian Amazonia, it drains an area of approximately 2.2 million km^2 (Latrubesse & Franzinelli, 2002). It is estimated that the annual load of suspended sediment amounts to up to 700 million t (Dunne et al., 1998).

The floodplains influenced by the sediment-rich white-water rivers are called várzea (Sioli, 1954; Prance, 1979). The várzea covers an area of approximately 200,000 km^2, which is 4–5% of the Amazon basin (Junk, 1989; Hess et al., 2003). Due to the comparatively high nutrient content of its substrate and richness in natural resources, the várzea is the ecosystem most densely inhabited by humans within Amazonia (Junk & Piedade, 1997).

The high suspension load of the white-water rivers combined with generally low slopes (2–3 cm km^{-1}, Irion et al., 1997) over most of the Amazon basin result in meandering rivers and consequently a highly dynamic várzea landscape. The rivers are characterized by a monomodal flood-pulse (Junk et al., 1989), which is the result of precipitation seasonality in the greater part of the catchment area. In central Amazonia, flood amplitudes reach mean heights of up to 10 m, resulting in the periodical inundation of the adjacent lowlands. Therefore, the Amazonian várzea is characterized by a well-defined high-water period (aquatic phase) and a low-water period (terrestrial phase) during the year.

Amazonian white-water rivers undergo rapid spatial and temporal change, as erosion and deposition continually destroy and recreate fluvial forms (Kalliola et al., 1991). Next to the main-river channel of the Ucayali–Solimões–Amazon River, sedimentation on point bars can reach 0.3–1 m year^{-1} (Junk, 1989; Campbell et al., 1992). On undercut slopes, erosion can wash out several hectares of forest during a single high-water period (Wittmann et al., 2004). The unstable habitat conditions caused by the processes of sedimentation and erosion result in a highly diverse patchwork of microhabitats (Campbell et al., 1992), which is reflected by the vegetation cover. In general, sedimentation and substrate texture are linked to both the distance of the sites from the main-river channels and the period of inundation to which the sites are subjected (Mertes et al., 1995; Wittmann et al., 2004). Water current is highest next to the main-river channels, where sedimentation rates are high and relative coarse fractions, such as sand, are deposited at fluvial islands and river banks. With increasing distance from the rivers, current energy is reduced by the

* Corresponding author. Tel./fax: +49 (xx55) 92 36421503.
E-mail address: F-Wittmann@web.de (F. Wittmann).

0034-4257/$ – see front matter © 2009 Elsevier Inc. All rights reserved.
doi:10.1016/j.rse.2009.06.015

water resistance posed by levees and the vegetation cover, resulting in decreased sedimentation rates. Simultaneously, fine grains, such as silt and clay, are deposited, especially when the floodwaters are non-turbulent and persist for several weeks or months in oxbows, lakes, and backwater depressions.

Approximately 75% of the várzea is covered by forest. Várzea forests are the most species-rich floodplain forests worldwide (Wittmann et al., 2006). Besides comparatively long floristic evolution since at least the Paleocene (Kubitzki, 1989), it is thought that the exceptional tree species richness in Amazonian várzea can be traced back to the high beta-diversity of the alluvial landscape (Salo et al., 1986; Campbell et al., 1992; Marston et al., 1995) in combination with a moderate disturbance regime imposed on plant assemblages by the annual floods. The distribution of the different várzea forest types is thus determined by adaptations of tree species to different levels and periods of flooding, and most habitats and species are strongly zoned along the flooding gradient (Junk, 1989; Ayres, 1993; Wittmann et al., 2006).

In contrast to undisturbed Amazonian upland forests, where tree regeneration commonly starts in small to medium-sized gaps caused by the mortality of single trees, or collapse of groups of trees in the top canopy, the fluvial dynamism in the várzea continuously creates large areas for new-site colonization. The small-scale changes of sedimentation rates and substrate texture directly influence the distribution of tree species and forest types (Wittmann et al., 2004). On the one hand, drainage in coarse-grained soils is better than in fine-grained soils, where oxygen is rapidly consumed due to the decomposition of accumulated organic matter by microorganisms (Larcher, 1994). On the other hand, sites with coarse-grained substrates normally undergo high sedimentation rates, which impede tree regeneration and cover superficial root layers of mature individuals. Only a few pioneer plants are able to tolerate these environmental conditions, i.e. grasses such as *Echinochloa polystachya* and *Paspalum* spp., and few tree species such as *Alchornea castaneifolia*, *Salix martiana*, and *Cecropia latiloba* in central Amazonian várzea (Wittmann et al., 2004), and *Tessaria integrifolia* in western Amazonian várzea (Lamotte 1990; Kalliola et al., 1991).

The ecologic consequences of river channel migration and alluvial land forms for the biota of the várzea floodplains are still poorly understood (Richards et al., 2002). Studies based on both local measurements and remotely sensed data reported increasing geomorphic activity of the Ucayali–Solimões–Amazon River from central Amazonia toward the western part of Amazonia (Salo et al., 1986; Almeida, 1989; Mertes et al., 1996; Rozo et al., 2005). It is well-known that new-site colonization of freshly deposited sediment by pioneer forest and forest succession within the várzea floodplain strongly depend on the geomorphic dynamism of the white-water rivers (Salo et al., 1986; Kalliola et al., 1991; Campbell et al., 1992). But it is largely unknown to what extent erosion and deposition along the main-river channels affects forest coverage in spatial and temporal scales. However, this knowledge is fundamental for the comprehension of ecosystem processes, e.g., biodiversity modeling and ecosystem fluxes, the monitoring of aboveground woody biomass, and its extrapolation to ecosystem or biome-wide carbon cycle modeling.

In this study, we quantified and monitored alluvial erosion, deposition, river channel migration, and their impact on the distribution of várzea forest types along river bank transects of the Japurá and the Solimões Rivers, western Brazilian Amazonia, by remote-sensing techniques over a 21-year period. The aim of this study was to test whether the geomorphic dynamism of the rivers in this part of the Amazon basin influences the creation and distribution of vegetation types, if variability of erosion and deposition existed over the studied period, and if the ratio erosion/deposition leads to gains or losses of area potentially suitable for vegetation colonization in the studied region. In addition, we use local biomass and carbon-stock estimates of the várzea vegetation to discuss how the geomorphic dynamism of the Japurá and Solimões Rivers influences the carbon-budget of the várzea in this part of the Amazon basin.

2. Methods

2.1. Study area

The study was performed within the Mamirauá Sustainable Development Reserve (MSDR, 02°48′–02°54′ S, 64°53′–65°03′ W), located approximately 550 km W of the city of Manaus, western Brazilian Amazon (Fig. 1). The MSDR is delimited by the Solimões, Japurá and Auati Rivers, the latter being a channel that connects the Solimões to the Japurá River. The MSDR has a size of approximately 1,124,000 ha, and is divided in a subsidiary area (864,000 ha), and a focal area (260,000 ha), separated from each other through a river channel named Aranapu (Fig. 1, Sociedade Civil Mamirauá, 1996).

The entire reserve is located on the Plio-Pleistocene Içá Formation, which is covered by unconsolidated alluvial sediment of the Solimões and the Japurá rivers (Rossetti et al., 2005). Mean monthly temperatures in the MSDR vary a little over the year and range between 25 and 28 °C, mean annual rainfall amounts to approximately 3000 mm (Wittmann & Junk, 2003).

Annual water-level fluctuations of the Solimões and Japurá Rivers averaged approximately 11 m since 1993 (Institute for Sustainable Development Research at Mamirauá — ISDRM). Variations in geomorphology, pedology, and the vegetation cover of the MSDR are directly related to the mechanisms of deposition and fixation of the alluvial substrate. Next to the river banks, eutrophic substrates are mainly composed of fine sand, whereas silt- and clay-rich hydromorphic gleys dominate further inland. The substrate clay fraction in the MSDR ranges from approximately 30% at the river banks up to 83% further inland (Wittmann et al., 2004). Due to the high variability of the hydraulic relations within the extensive floodplain, the landscape of the MSDR is a patchwork of recent fluvial linear channel-bars that are intercalated with levees, ancient channel-bars, oxbows, and lakes, periodically interconnected with each other and the main-river system (RADAMBRASIL, 1977). About 90% of the focal area of the MSDR is covered by different forest types (Sociedade Civil Mamirauá, 1996). The vegetation cover near the lower banks of the river channels is dominated by aquatic and semi-aquatic macrophytes (herbaceous grasses, with dominance of *E. polystachya* and *Paspalum* spp.), and the pioneer tree species *A. castaneifolia, S. martiana* and *C. latiloba*, which mostly form mono-specific stands (Wittmann et al., 2002, 2004). These pioneer tree species establish at mean maximum flood-levels of approximately 5–7 m water depth, and their stems and aboveground roots secure the deposited alluvial sediment (Wittmann et al., 2004). Floristic inventories in combination with tree-age determinations derived through dendrochronological methods indicate that mean maximum stand ages of pioneer forest types is about 10–15 years when dominated by *A. castaneifolia* and *S. martiana*, whereas it is about 25 years when dominated by *C. latiloba* (Worbes et al., 1992; Schöngart 2003). These pioneer forest types were estimated to cover 29% of the focal area of the MSDR (Wittmann et al., 2002).

2.2. Image processing and mask choice

The study was performed utilizing Landsat 5 Thematic Mapper (TM) image data for the scene at path 1, row 62, provided by the National Institute for Space Research — INPE. Four of the sensor's bands were employed: 3 (red), 4 (near-infrared), 5 (mid-infrared) and 7 (mid-infrared). We acquired six images of this scene, all dating to periods at or near low-water stage (September–November), between 1984 and 2005 (Table 1). At our study site, water levels of the rivers recede beginning in mid June to early July. Water-level minima generally occur between October and November (IBGE, 1991). Only images with cloud cover <20% were used.

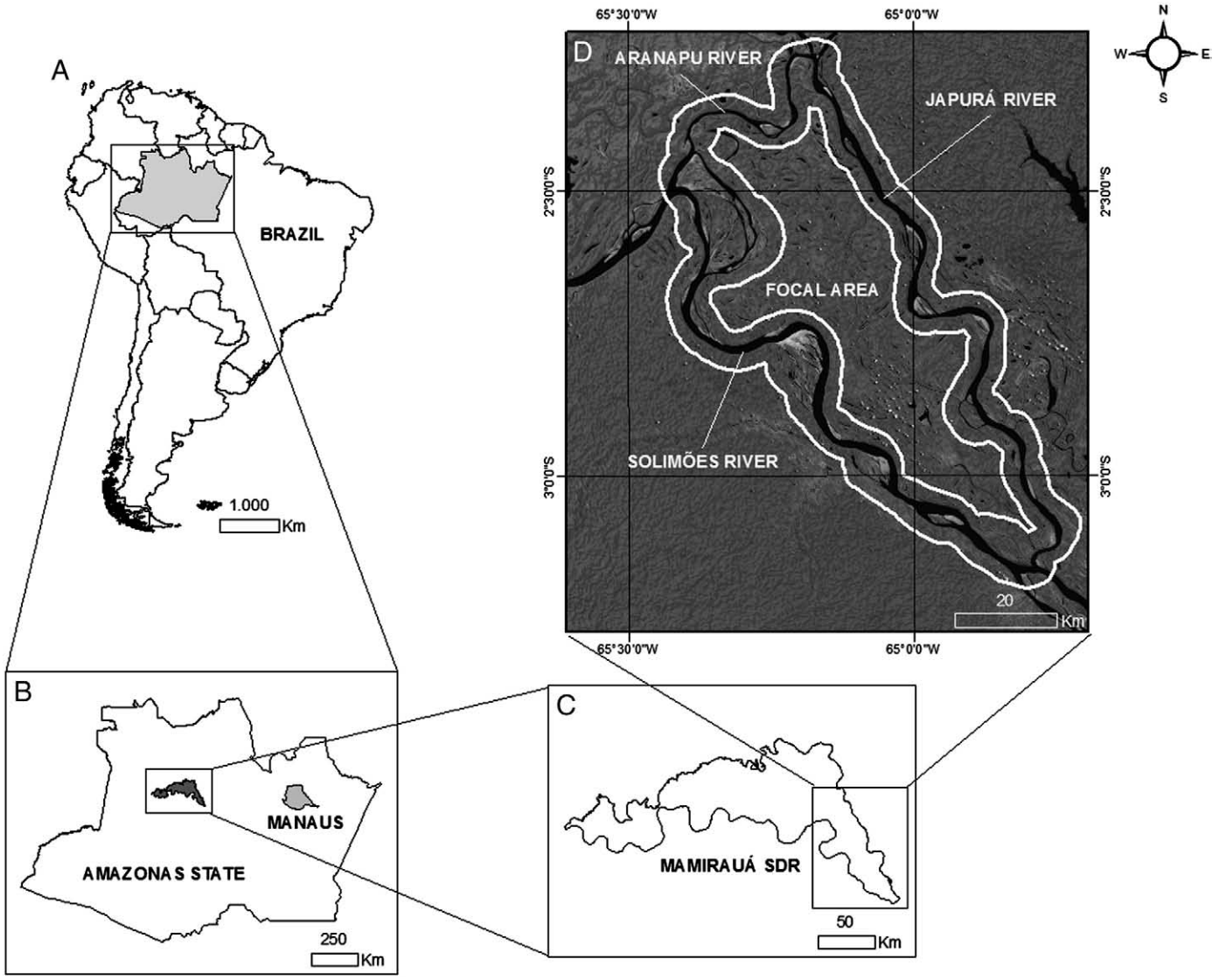

Fig. 1. Location of the focal area of the Mamirauá Sustainable Development Reserve (C), within the State of Amazonas, Brazil (A, and B), and the study area (in white) along the banks of the Solimões, Japurá, and Aranapu Rivers (D).

The images were georeferenced using the ortho-rectified Landsat Thematic Mapper Compressed Mosaics (GeoCover™), which have an RMS error of 50 m. All bands of each date were converted from quantized radiance values to reflectance values, using the method described by Chen and Herz (1996). In order to reduce distortions from variable atmospheres, different sun-elevation angles and from sensor degradation over time, linear radiometric normalization of all bands was performed, using the 1986 image as calibration standard. The sensor was new and atmosphere was relatively clear for the 1986 date. Band 3 of the 1986 image was first atmospherically corrected following the COST model of dark-object subtraction (Chavez, 1996). Longer wavelengths are less affected by aerosols, so the three optical infrared bands of the 1986 image were used without atmospheric correction. Following the method of Roberts et al. (2002), invariant bright and dark objects were selected in each band's image for each pair of dates: the 1986 radiometric standard and the date undergoing relative radiometric correction.

The river banks delimitating the focal area of the MSDR were digitized, creating a vector data layer containing the shape of the three open water river channels in 1984. Because bank accretion and erosion did not surpass 3 km during the 21-year period, all areas more than 3 km inland from the 1984 channel margins were masked out, leaving a pre-selected study area (Fig. 1). All clouds and cloud shadows found at any of the six dates were added to the mask. Clouds and their shadows covered 44% of the pre-selected study area (Table 1), which resulted in a final cloud-free study area of 153,032 ha. The 3 km buffer was arbitrary, so the cloud-free open-channel area of each river was used to normalize rates of annual lateral accretion, lateral erosion and channel migration (Mertes et al., 1996).

Table 1
Landsat 5 TM image data (path/row 1/62, bands 3, 4, 5, and 7); water-level variability of the Solimões River at the study site; and cloud cover.

Landsat 5 TM	Water level (m asl)	Cloud cover (%)
26/09/1984	22.51	3.9
18/10/1986	21.47	11.0
05/10/1993	21.51	19.3
14/09/1997	20.44	12.8
25/11/2000	19.58	5.0
04/09/2005	20.14	2.7
Std dev.	1.07	–
Temporal composite	–	44

Images from Brazil's National Institute for Space Research (INPE), water levels provided by the Manaus Harbor Authority (Capitania dos Portos).

The variation of low-water stages between years (Table 1) caused variable exposure of un-vegetated beach, bar and river-bed surfaces that would lead to errors in the estimates of lateral erosion and accretion. We eliminated this problem by considering bank erosion and accretion to be, respectively, the loss or appearance of vegetated surfaces. This procedure also tolerates some small variation in the level of flooding under the canopy of vegetation on newly deposited surfaces, as long as the canopy is closed and not completely submerged. Some error is introduced by classifying floating vegetation in backwaters as being vegetated land, but this error is small because the floating vegetation is greatly reduced at low-water stage.

For each image date it was therefore necessary to differentiate vegetated land from all other features, namely water and non-vegetated land. Water was identified using a threshold reflectance value of Landsat band 7. Land surfaces without green vegetation were identified using a threshold value of the *Aerosol Free Vegetation Index* — $AFRI_{2.1}$ (the subscript refers to the TM band 7 wavelength). This index has the advantage of being scarcely influenced by the atmospheric aerosol-content (Karnieli et al., 2001). After applying the two thresholds, a thematic map containing two classes – vegetation and non-vegetation – was created for each date: 1984, 1986, 1993, 1997, 2000 and 2005.

2.3. Quantification of lateral accretion, erosion, and river channel migrations

The ISDRM has daily water-level records of the Solimões River in Tefé only since 1993. As our investigation period starts before that, we obtained the water levels for each image date from the daily records of the Negro/Solimões River in the harbor of Manaus, which are available since 1903. Despite the distance of 550 km, Manaus shows strong correlation with the water levels in the MSDR, with a difference of only 9 cm in the mean amplitude (Schöngart et al., 2005). The range of water levels over the six dates was 2.93 m (Table 1).

The detection of channel migrations, lateral accretion and lateral erosion were based on the identification of pixel class-changes in five pairs of successive dates (Table 2). In each of the five time periods, three change classes were recognized: (1) erosion (changes from vegetation to non-vegetation), (2) lateral accretion (changes from non-vegetation to vegetation), and (3) no change. The five time intervals ranged from two to seven years, so erosion and accretion were standardized to annual rates. Dynamic areas were those whose initial class changed at least once during the five intervals. Stable areas were defined as those where no class-changes occurred.

A channel migration value (Mertes et al., 1996) was derived for each of the three major river reaches that border the MSDR: the Solimões and Japurá Rivers, and the Aranapu channel. Channel migration values were computed as the total vegetated land areas eroded and deposited, divided by the area of cloud-free open water body along a reach at 1984 low-water stage, divided by the number of years. The units are "percent change per year". Cloud-free pixels must have no clouds or their shadows in all six image dates. Cloud-free open water river channels totalled 37,217 ha for the entire study area, partitioned among the Solimões (20,717 ha), Japurá (12,921 ha) and Aranapu (3679 ha). Thalweg lengths were 140 km, 126 km and 43 km, respectively.

2.4. Changes in vegetation cover

Changes in vegetation cover were based on a previous vegetation classification scheme in the same study area by Wittmann et al. (2002). As vegetation colonizing the newly deposited banks consists of pioneer plants with mean maximum stand age of 25 years, we restricted the investigation on vegetation changes to the period 1984–2005.

A supervised maximum-likelihood classification at probability-levels of 0.7 was applied in the study area, using bands 3, 4, 5, and 7, in 1984 and 2005. Two cover classes were defined: 1) Pioneer vegetation (P_{Veg}) on freshly deposited sediment (herbaceous macrophytes, and mono-dominant forest, mainly composed of *S. martiana*, *A. castaneifolia*, and *C. latiloba*), and 2) later successional forest (L_{Veg}, all other forest types). Due to significant differences in tree heights, single crown areas, and canopy roughness, these two vegetation types show distinct reflectance patterns and thus are easy to classify (Wittmann et al., 2002). The classification in 2005 was based on GPS-georeferenced training sites that were equally distributed in P_{Veg} and L_{Veg}, obtained in the field during the period 2000–2005 (Fig. 3A). Texture and spectral pattern of these training sites was investigated quantitatively and qualitatively by visual image analysis, and the classification afterwards applied also to the 1984 image. Gains and losses of areas covered by P_{Veg} and L_{Veg} were quantified by image subtraction.

3. Results

3.1. Lateral accretion, erosion, and river channel migration

During the period of 21 years, 7.9% of the study area (12,025 ha) changed at least once from the 1984 class. Pixels may have changed classes two or more times within a single time interval and thus were wrongly classified as non-change class, especially when the time period between a pair of consecutive images extended over several years. However, these undetected multiple changes within a single interval were uncommon, because pixels undergoing multiple changes detected across two or more time intervals occurred in less than 1% of the studied area.

The rates of accretion and erosion were well-balanced during the 21-year period. Floodplain accretion represented 51.4% of the pixel class-changes, whereas eroded areas represented 48.6% (Table 2). Over the 21 years, annual lateral accretion rate averaged 0.83% and erosion averaged 0.79% of the cloud-free open water area, or 310 and 294 ha $year^{-1}$, respectively (Table 2). Lateral accretion exceeded erosion in the intervals 1984–1986, 1986–1993 and 1997–2000. Erosion was higher for 1993–1997 and 2000–2005 (Table 2). Most

Table 2
Amounts (ha) and annual rates (% of cloud-free open-channel water area) of lateral accretion and erosion of vegetated land for each of the five time intervals.

Sequence	Time interval	Period (years)	NC	Accretion			Erosion		
			ha	ha	ha $year^{-1}$	% $year^{-1}$	ha	ha $year^{-1}$	% $year^{-1}$
1	1984–1986	2	151,526	782	391	1.05	724	362	0.97
2	1986–1993	7	148,349	2509	358	0.96	2174	311	0.83
3	1993–1997	4	151,124	866	217	0.58	1042	261	0.70
4	1997–2000	3	150,982	1249	416	1.12	801	267	0.72
5	2000–2005	5	150,498	1109	222	0.59	1425	285	0.76
Weighted means					310	0.83		294	0.79
Sums				6515			6166		

Accretion slightly exceeded erosion over the 21 years. NC = no-change areas.

Table 3
Percent channel migration (CM) per year and areas of accretion (*A*) and erosion (*E*) of each of the three river segments for each of the five time intervals and for the full 21 years.

Sequence	Interval	Period (years)	Solimões			Japurá			Aranapu		
			CM (%)	*A* (ha)	*E* (ha)	CM (%)	*A* (ha)	*E* (ha)	CM (%)	*A* (ha)	*E* (ha)
1	1984–1986	2	2.5	601	423	1.3	164	173	2.0	17	128
2	1986–1993	7	1.8	1405	1143	1.5	786	561	3.1	318	470
3	1993–1997	4	1.4	438	709	0.9	284	160	2.1	144	173
4	1997–2000	3	2.0	692	541	1.2	373	90	3.2	184	170
5	2000–2005	5	1.6	935	709	0.8	117	426	1.9	57	290
Entire 21 years	1984–2005	21	1.8	4071	3525	1.2	1724	1410	2.5	720	1231

CM = 100 * (annual *A* + annual *E*) / (cloud-free channel area).

land-changes were restricted to point bars along the river channels, with fewer landform changes on fluvial islands.

Channel migration values (annual erosion plus annual accretion expressed as a percent of the cloud-free open water area of each river reach for the 21-year period) amounted to 1.8% year^{-1} for the Solimões River, 1.2% year^{-1} for the Japurá River, and 2.5% year^{-1} for the Aranapu channel (Table 3). Channel migrations differed considerably in space, both within and between the three main-river channels. They were highest at the confluence of the Solimões and Aranapu Rivers (Fig. 2). Lateral accretion generally exceeded erosion along the Solimões and Japurá Rivers, whereas erosion exceeded deposition along the Aranapu channel.

3.2. Changes in vegetation cover

The vegetation types (P_{Veg}, and L_{Veg}) could easily be classified by maximum-likelihood clustering, as indicated by kappa-coefficients of 96% in 1984 and 98% in 2005. However, it was not possible to differentiate between grasses and pioneer trees in P_{Veg}, or between different successional stages in L_{Veg}. In P_{Veg}, herbaceous plants and pioneer trees were characterized by similar reflectance patterns, especially when trees were in the juvenile phase and had still not formed closed canopies. On the other hand, different successional stages in L_{Veg} always formed closed canopies, but structural patterns influencing reflectance values in the upper canopy, such as increasing

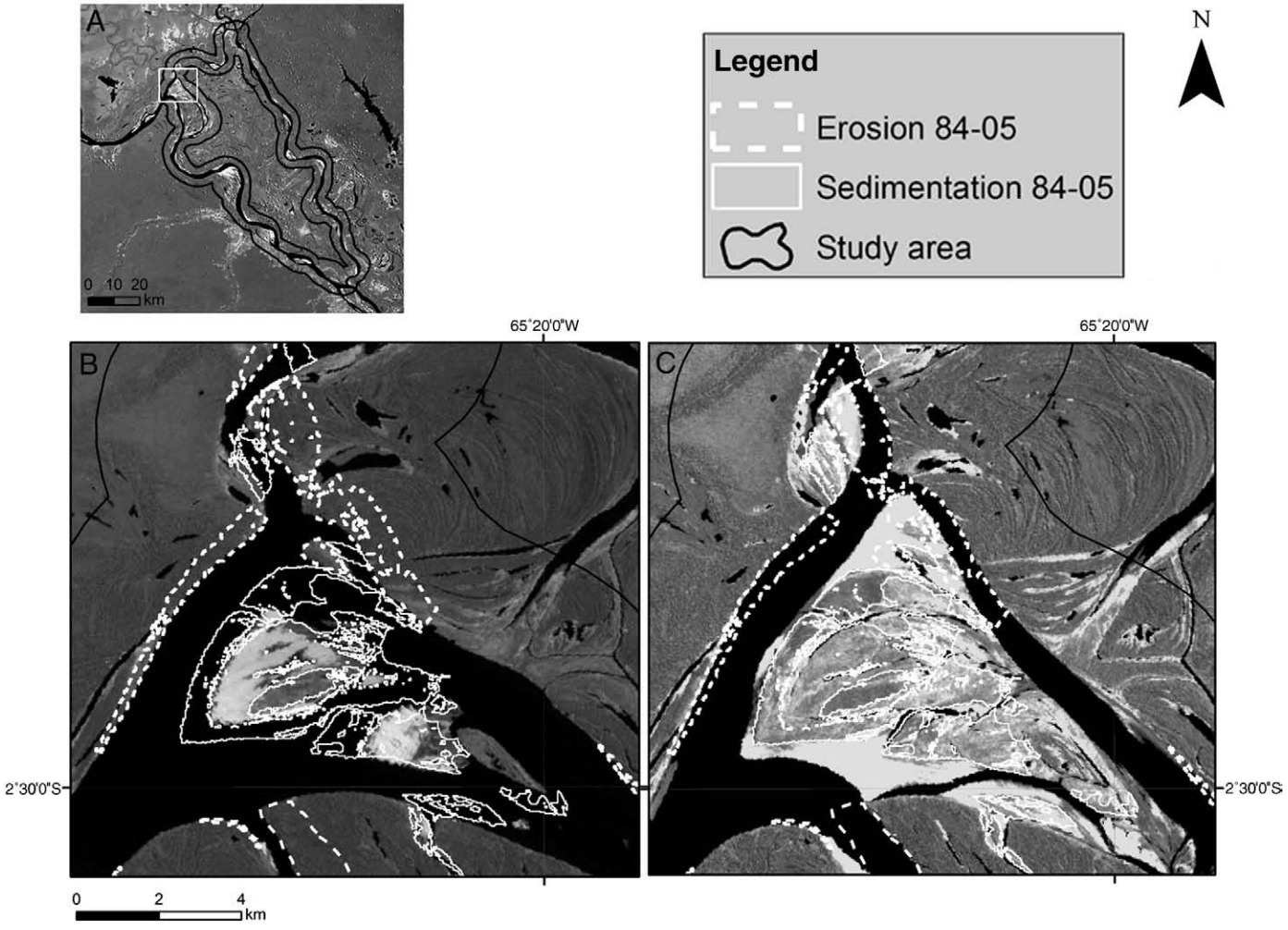

Fig. 2. Point bar formation at the confluence of the Solimões River and the Aranapu channel. Left side: 1984, right side: 2005.

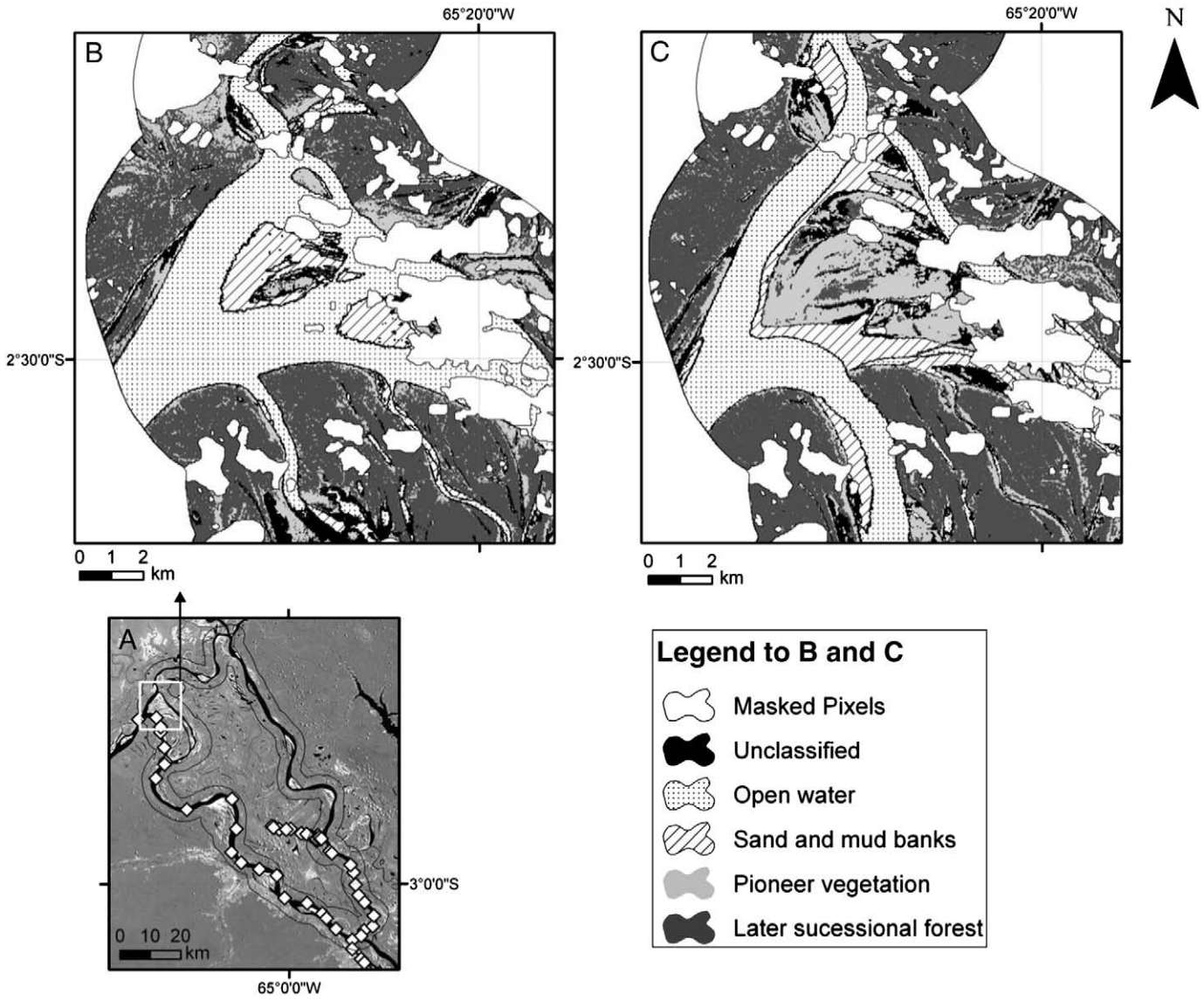

Fig. 3. Training sites along river banks and forests of the Japurá and Solimões Rivers, and the focal area of the Mamirauá Sustainable Development Reserve (A); and vegetation changes at the confluence of the Solimões and the Aranapu River channels between 1984 (B) and 2005 (C).

tree heights and crown sizes with increased stand ages (Wittmann et al., 2002; Schöngart 2003) are subtle and only classifiable with higher resolution optical sensors (Wittmann et al., 2002).

In 1984, the P_{Veg} occurred on an area of 12,080 ha (7.9% of the study area), and the L_{Veg} on an area of 82,600 ha (54%). In 2005, the area covered by P_{Veg} had nearly doubled to 21,000 ha (13.7% of the study area), whereas the area covered by L_{Veg} dropped to 74,160 ha (48.5%, Fig. 3). Gains in P_{Veg} (5.8% of the study area) were balanced by losses of L_{Veg}, (5.5% of the study area). While erosion of L_{Veg} mainly was restricted to undercut slopes along the main-river channels, newly established P_{Veg} again concentrated on point bars, with highest colonization rates near the confluences of the rivers and channels (Fig. 3).

4. Discussion

Different types of image data, different methods and even different concepts of change have been employed in past studies that monitored and mapped fluvial channel dynamics. This makes comparison difficult. Most studies have used the Landsat series of optical orbital sensors: MSS, TM and ETM (Almeida, 1989; Kalliola et al., 1991, 1992; Rozo et al., 2005; Salo et al., 1986), sometimes complemented with data from topographic maps, navigational charts and ship's logs (Almeida, 1989; Mertes et al., 1996).

The multi-temporal analysis of Landsat 5 TM image data allowed for the detection and the monitoring of erosion and deposition along the river channels of the MSDR, and for a rough classification of two várzea vegetation types. Multi-spectral TM images are still a convenient and economical remote-sensing resource for classifying and monitoring the várzea landscape. However, the utilization of multi-temporal optical image data in the Amazon basin is strongly affected by cloud cover, and cloudless scenes are scarce (Costa et al., 1998). In the present study, the cloud coverage summed over six dates of a single TM scene reduced our effective study area by 44%. TM image data thus provide important information about the *status quo* of landscapes, but their utilization in landscape monitoring over consecutive years is restricted to local patches that remain cloudless.

Alluvial geomorphology of the white-water rivers in the region of the MSDR was highly dynamic. Our results indicated that the major part of temporal comparisons along the Solimões and Japurá Rivers show higher sedimentation than erosion activity, whereas erosion exceeded deposition along the Aranapu channel; however these ratios

Table 4
Studies that monitored river channel migrations of white-water rivers across equatorial Amazonia.

Reference	Data	River	Latitude/longitude	Transect size km (km^2)	Period	CM ($year^{-1}$)
Salo et al. (1986)	Landsat MSS	Manu — Peru	11°53′/12°15′ S 71°24′/70°55′ W	70 (325)	1962/63–1979	12 m
Kalliola et al. (1991)	Landsat MSS	Ucayali — Peru	4° to 9° S/72° to 77° W	90 (–)	1979–1983	2.6 km^2
Kalliola et al. (1992)	Landsat MSS	Ucayali–Marañon–Amazon (Solimões) river system — Peru	4°30′S/73°30′W	0.7 (channel width)	07/30/1979 to 09/19/1983	14–23%
Mertes et al. (1996)	SLAR	Solimões — Brazil	1° to 4° S/65° to 68° W	100 (225)	1971/72–1979/80	0.8%
Rozo et al. (2005)	Landsat TM, ETM	Amazon — Brazil	2°59′51″/3°30′11″ S, 58°43′52″/59°54′14″ W	130 (757)	1986–2001	0.002%
This study	Landsat TM	Solimões — Brazil	02°48′/02°54′ S 64°53′65°03′ W	140 (207)	1984–2005	1.8%
This study	Landsat TM	Japurá — Brazil	64°53′/65°03′ W	126 (129)		1.2%
This study	Landsat TM	Aranapu — Brazil		42 (36.8)		2.5%

CM = channel migration.

were well-balanced when monitored over the whole study period of 21 years. Compensation between deposition and erosion occurs, however, in different proportions between the studied river transects. Channel adjustment is considerably greater along the Solimões than on the Japurá River. The main reason for higher dynamism of the Solimões River can be traced back to its catchment area in the central part of the Andes in Peru and Ecuador, where precipitation, weathering, and erosion are extreme (IBGE 1991; Irion, 1984; Sioli, 1984). The Solimões River flows through the extensive equatorial formation of Tertiary and Quaternary sediments, with the most part of its affluents originating from this formation. Hydrological measurements of water discharge and suspended solid contents of the Solimões River performed by Abdo et al. (1998) near the city of Fonte Boa (approximately 100 km W of our study site) indicated a water discharge of 71,810 $m^3\ s^{-1}$, the suspended sediment load amounting to 66.7 mg l^{-1}. By contrast, the Japurá River originates from the northern part of the Andes in Colombia and Venezuela. Water discharge above its confluence with the Solimões River, near the city of Maraã, amounts to approximately 17,000 $m^3\ s^{-1}$, and the suspended sediment load to approximately 31.0 mg l^{-1} (Abdo et al., 1998). Many of the northern affluents of the Japurá River consist of sediment- and nutrient-poor black-waters that originate from the northern Amazonian Precambrian Guayana shield. Smaller discharge combined with less content of suspended solids is thus the main reason for lower alluvial dynamism of the Japurá River.

Differences in the intensity of geomorphic changes between these two rivers may also depend on variable valley sizes and the MSDR being located at their confluence. In general, the dominance of lateral or of overbank floodplain-forming processes varies spatially as valley slope and unit stream energy decline (Sioli, 1984; Hudson, 2003). Valley deposits represent topographic and sedimentary controls on contemporary flood processes, with the height of the meander belt being the dominant topographic control above the floodplain bottoms (Hudson & Colditz, 2003). According to Latrubesse (2008), both the Japurá and Solimões Rivers are among the nine largest rivers on Earth, and can be classified as 'anabranching mega rivers', which have relatively straight courses. However, both the Solimões and Japurá Rivers build meanders in their upper reaches. While the lower Japurá River still tends to meander above its confluence with the Aranapu, the Solimões River here is approaching the transitional zone to its mid-basin, characterized by the formation of fewer meanders (Sioli, 1984). This may be related to different slopes, which are generally higher along the Japurá River than along the Solimões River in this part of the basin (3.6–4.1 cm km^{-1} and 1.6–3.8 cm km^{-1}, respectively, Latrubesse 2008). However, meanders also reduce hydraulic energy along the lower Japurá River, which could explain the generally higher geomorphic dynamism along the Solimões River.

Intense deposition and erosion activity along the Solimões River directly affects rates of channel migration. The rate of channel migration recorded along the Solimões River (1.8% $year^{-1}$) is greater than that reported by Mertes et al. (1996) for the same river and region (0.8%). These authors also reported lateral channel migrations of the Solimões River of up to 140 m $year^{-1}$ (corresponding to 3% $year^{-1}$) near the city of Fonte Boa. In general, fluvial dynamics of the Solimões River seems to increase exponentially towards the headwaters, from eastern to western Amazonia (Table 4). While Almeida (1989) and Rozo et al. (2005) found a high geometric stability of the channel-bars of the middle Amazon and lower Madeira rivers, with channel migrations of only 0.002% $year^{-1}$ between Careiro Island near the city of Manaus and the confluence of the Amazon and Madeira Rivers, Kalliola et al. (1992) reported channel migrations of up to 37% $year^{-1}$ along the Peruvian Amazon River (Table 4). From their study along a 70 km long transect bordering the Manu River in Peruvian Amazonia, Salo et al. (1986) stated that 26.6% of Peruvian várzea forests are characterized by recent processes of erosion and deposition. Kalliola et al. (1991) reported fluvial erosion of 260 ha during a period of 4 years along a 90 km long transect bordering the Ucayali River (Peruvian Amazon), with simultaneous deposition of 270 ha of channel-bars subject to colonization by pioneer vegetation. The authors stated that the geomorphic dynamism is especially pronounced in western Amazonian várzea, where mosaics of lakes and floodplains are intercalated with inter-fluvial streams, which in turn promote the extreme geomorphic variations in the seasonally flooded landscape.

Channel migrations along the investigated rivers were mostly concentrated on point bars that are located next to river meanders and at the confluence between the main-river and river channels (Fig. 2). According to Mertes et al. (1995, 1996), point bars are extremely unstable and most likely to migrate laterally when intercepted by secondary channels. Frequently, the migration of point bars leads to the creation of fluvial islands.

Continuous channel migration and the deposition of sediment are crucial factors influencing the vegetation cover within the várzea (Salo et al., 1986; Kalliola et al., 1991; Sternberg, 1998; Richards et al., 2002; Wittmann et al., 2004). The geomorphic dynamism of the white-water rivers induces a natural ecosystem disturbance which is the prerequisite to maintain early stages of vegetation succession along the river channels. In combination with reduced alluvial dynamics further inland, i.e., near backwater depressions and lakes, alluvial disturbance next to the main-river channels contributes to high beta-diversity and exceptional tree species richness within Amazonian várzea (Campbell et al., 1992; Wittmann et al., 2006). High alluvial dynamic in this part of the Amazon basin thus contributes to general higher species richness of várzea forests in comparison to those located further east, where geomorphic dynamism is reduced. Indeed, the highest tree species richness was reported for floodplain forests of the upper Amazon (Wittmann et al., 2006), which is also the region subject to highest geomorphic dynamic.

The results of our study indicate that the white-water rivers bordering the MSDR annually deposit an area of approximately 425 ha

subjected to colonization by early-succession species. During the 21-year study, pioneer vegetation in our study site was established on a total area of 8920 ha. The biomass of this pioneer vegetation can roughly be estimated based on local biomass determinations performed by Piedade et al. (1991) and Morison et al. (2000) for herbaceous plants (total biomass) and Schöngart (2003) for pioneer forest (aboveground wood biomass). According to these authors, total biomass of the herbaceous vegetation amounts to approximately 100 Mg ha^{-1}, and the aboveground wood biomass of pioneer forest is 15–217 Mg ha^{-1} (depending on forest stand age between 0 and 25 years, and depending on the allometric equation used). These data suggest that new-site colonization by pioneer vegetation adds 6371–92,173 Mg $year^{-1}$ to biomass stocks in our study area. Assuming that half of biomass normally is stored in the form of carbon (Fearnside & Guimarães, 1996; Bernoux et al., 2001), carbon sequestration by new-site creation at our study site thus ranges between 3185 and 46,086 Mg $year^{-1}$. As sediment deposition and erosion were well-balanced in our study, the creation of areas suitable for colonization by pioneer plants implies the natural erosion and destruction of other forest types. At our study site, the area covered by late-successional forest was reduced by 8840 ha during the 21-year period (421 ha $year^{-1}$). Aboveground wood biomass in this forest amounts to 108–307 Mg ha^{-1} (Schöngart, 2003; depending on the stand age, and the allometric equation used). Carbon releases by alluvial erosion in our study site thus would range 22,734–64,623 Mg $year^{-1}$. These values suggest that C-releases by alluvial dynamics would be much higher than C-sequestration at our study site. However, our estimate does not take into account biomass sequestration that occurs after early-successional stages develop into later successional forest. Moreover, the channel migration rates detected at the three river channels suggest that all forest types may be subject to erosion, independent of their successional stage. There is no evidence that the spatial distribution of vegetation types within the MSDR was subject to significant changes during the last decades. The water-level records at the harbor of Manaus since 1903 did not also indicate significant anomalies in the flooding behavior of the Solimões River (Schöngart & Junk, 2007), nor increased erosion activity during the past years. However, the unbalanced C-budget in our rough estimate indicates that alluvial erosion and deposition processes maybe subject to cyclic variability, which is yet poorly understood.

Acknowledgements

We wish to thank the Mamirauá Institute for Sustainable Development Research (ISDRM) for the assistance, and the Brazilian Research Council (CNPq) for the first author's graduate student fellowship. Field work was supported by the INPA/Max Planck Project, Manaus. We thank three unknown referees for their valuable comments on this manuscript.

References

Abdo, J. M. M., Benevides, V. F. S., Coimbra, R. M., Oliveira, E., Lourd, M., & Fritsch, J. M. (1998). *Oitava campanha de medição de vazão e amostragem de água e sedimentos na bacia do Rio Solimões e no Rio Amazonas. Hidrologia da bacia Amazônica* (HiBAm). *ORSTOM-CNPq, Aneel. Brasília: UNB*.

Almeida, W. S. (1989). *Metodologia de sensoriamento remoto no monitoramento de modificações no canal fluvial e atualização de cartas náuticas*. Dissertation, Instituto Nacional de Pesquisas Espaciais, São José dos Campos, Brazil.

Ayres, J. M. (1993) As matas de várzea do Mamirauá, In Sociedade Civil Mamirauá (Ed.), Estudos de Mamirauá (pp. 1–123). Brasília: MCT/CNPq.

Bernoux, M., Graça, P. M. A., Cerri, C. C., Fearnside, P. M., Feigl, B. J., & Piccolo, M. C. (2001). Carbon storage in biomass and soils. In M. E. McClain, R. L. Victoria, & J. E. Richey (Eds.), *The biogeochemistry of the Amazon Basin* (pp. 165—184). London: Oxford University Press.

Campbell, D. G., Stone, J. L., & Rosas, A. (1992). A comparison of the phytosociology and dynamics of three floodplain (várzea) forests of known ages, Rio Juruá, western Brazilian Amazon. *Botanical Journal of the Linnean Society*, *108*, 213—237.

Chavez, P. S., Jr. (1996). Image-based atmospheric corrections — Revisited and improved. *Photogrammetric Engineering and Remote Sensing*, *62*(9), 1025—1036.

Chen, S. C., & Herz, R., (1996). Estudos quantitativos e calibração radiométrica de dados digitais do Landsat-5. In Instituto Nacional de Pesquisas Espaciais/Imagem Multimídia (Ed.) *Anais do VIII Simpósio Brasileiro de Sensoriamento Remoto, Salvador*. CD-ROM publ., São Paulo, Brazil

Costa, M. P., Novo, E. M., Ahern, F., Mitsuo, F., Mantovani, J. E., Ballester, M. V., et al. (1998). The Amazon floodplain through radar eyes: Lago Grande de Monte Alegre case study. *Canadian Journal of Remote Sensing*, *24*, 339—349.

Dunne, T., Mertes, L. A. K., Meade, R. H., Richey, J. E., & Forsberg, B. R. (1998). Exchanges of sediments between the flood plain and channel of the Amazon River in Brazil. *Geological Society of America Bulletin*, *110*, 450—467.

Fearnside, P. M., & Guimarães, W. M. (1996). Carbon uptake by secondary forests in Brazilian Amazonia. *Forest Ecology and Management*, *80*, 35—46.

Hess, L. L., Melack, J. M., Novo, E. M. L. M., Barbosa, C. C. F., & Gastil, M. (2003). Dual-season mapping of wetland inundation and vegetation for the central Amazon basin. *Remote Sensing of Environment*, *87*(4), 404—428.

Hudson, P. F. (2003). Floodplain styles of the lower Pánuco basin, Mexico. *Journal of Latin American Geography*, *1*, 58—68.

Hudson, P. F., & Colditz, R. R. (2003). Flood delineation in a large and complex alluvial valley, lower Pánuco basin, Mexico. *Journal of Hydrology*, *280*, 229—245.

IBGE — Fundação Instituto Brasileiro de Geografia e Estatística (1991). Geografia do Brasil — Região Norte. *Superintendência de Estudos Geográficos e Sócio-Econômicos Vol. 1* Rio de Janeiro, Brazil: Departamento de Geografia.

Irion, G. (1984). Sedimentation and sediments of Amazonian rivers and evolution of the Amazonian landscape since Pliocene times. In H. Sioli (Ed.), *The Amazon: Limnology and landscape ecology of a mighty tropical river and its basin* (pp. 201—214). Dordrecht: Dr W. Junk Publishers.

Irion, G., Junk, W. J., & Mello, J. A. (1997). The large central Amazonian river floodplains near Manaus: Geological, climatological, hydrological an geomorphological aspects. In W. J. Junk (Ed.), *The central Amazon floodplain: Ecology of a pulsating systemEcological Studies, vol. 126*. (pp. 23—46) Berlin: Springer.

Junk, W. J. (1989). Flood tolerance and tree distribution in central Amazonian floodplains. In L. B. Holm-Nielsen, I. C. Nielsen, & H. Balslev (Eds.), *Tropical forests: Botanical dynamics, speciation and diversity* (pp. 47—64). London: Academic Press.

Junk, W. J., Bayley, P. B., & Sparks, R. E. (1989). The flood pulse concept in river-floodplain systems. In D. Dodge (Ed.), *Proceedings of the International Large River Symposium, Ottawa. Canadian Special Publications of Fisheries and Aquatic Sciences*, *106*. (pp. 110—127).

Junk, W. J., & Piedade, M. T. F. (1997). Plant life in the floodplain with special reference to herbaceous plants. In W. J. Junk (Ed.), *The central Amazon floodplain: Ecology of a pulsing systemEcological Studies*, *vol. 126*. (pp. 223—265) Berlin: Springer.

Kalliola, R., Salo, J., Puhaka, M., & Rajasilta, M. (1991). New site formation and colonizing vegetation in primary succession on the western Amazon floodplains. *Journal of Ecology*, *79*, 877—901.

Kalliola, R., Salo, J., Puhakka, M., Rajasilta, M., Häme, T., Neller, R. J., et al. (1992). Upper Amazon channel migration: Implications for vegetation disturbance and succession using bitemporal Landsat MSS images. *Naturwissenschaften*, *79*, 75—79.

Karnielli, A., Kaufman, Y. J., Remer, L., & Wald, A. (2001). AFRI — Aerosol free vegetation index. *Remote Sensing of Environment*, *77*, 10—21.

Kubitzki, K. (1989). The ecogeographical differentiation of Amazonian inundation forests. *Plant Systematics and Evolution*, *163*, 285—304.

Lamotte, S. (1990). Fluvial dynamics and succession in the lower Ucayali River basin, Peruvian Amazonia. *Forest Ecology and Management*, *33/34*, 141—156.

Larcher, W. (1994). Ökophysiologie der Pflanzen. *Leben, Leistung und Streßbewältigung der Pflanzen in ihrer Umwelt* Stuttgart: UTB.

Latrubesse, E. M. (2008). Patterns of anabranching channels: The ultimate end-member adjustment of mega rivers. *Geomorphology*, *101*, 130—145.

Latrubesse, E. M., & Franzinelli, E. (2002). The Holocene alluvial plain of the middle Amazon River, Brazil. *Geomorphology*, *44*, 241—257.

Marston, R. A., Girel, J., Pautou, G., Piegay, H., Bravard, J. P., & Arneson, C. (1995). Channel metamorphosis, floodplain disturbance and vegetation development: Airn river, France. *Geomorphology*, *13*, 121—131.

Mertes, L. A. K., Daniel, D. L., Melack, J. M., Nelson, B., Martinelli, A., & Forsberg, B. R. (1995). Spatial patterns of hydrology, geomorphology, and vegetation on the floodplain of the Amazon River in Brazil from a remote sensing perspective. *Geomorphology*, *13*, 215—232.

Mertes, L. A. K., Dunne, T., & Martinelli, L. A. (1996). Channel-floodplain geomorphology along the Solimões–Amazon River, Brazil. *Geological Society of American Bulletin*, *108*(9), 1089—1107.

Morison, J. I. L., Piedade, M. T. F., Mueller, E., Long, S. P., Junk, W. J., & Jones, M. B. (2000). Very high productivity of the C4 aquatic grass *Echinochloa polystachya* in the Amazon floodplain confirmed by net ecosystem CO_2 flux measurements. *Oecologia*, *125*, 400—411.

Piedade, M. T. F., Junk, W. J., & Long, P. (1991). The productivity of the C_4 grass *Echinochloa polystachya* on the Amazon floodplain. *Ecology*, *72*(4), 1456—1463.

Prance, G. T. (1979). Notes on the vegetation of Amazonia III. The terminology of Amazonian forest types subject to inundation. *Brittonia*, *3*(1), 26—38.

RADAMBRASIL (1977). Levantamento dos Recursos Naturais. *Folha SA.19 Içá, Vol. 14* Rio de Janeiro, Brazil: Ministério das Minas e Energia, Departamento Nacional da Produção Mineral.

Richards, K., Brasington, J., & Hughes, F. (2002). Geomorphic dynamics of floodplains: Implications and a potential modeling strategy. *Freshwater Biology*, *47*, 559—579.

Roberts, D. A., Numata, I., Holmes, K., Batista, G., Krug, T., Monteiro, A., et al. (2002). Large area mapping of land-cover change in Rondonia using multitemporal spectral mixture and decision tree classifiers. *Journal of Geophysical Research*, *107*(D20), 8073.

Rossetti, D. F., Toledo, P. M., & Góes, A. M. (2005). New geological framework for Western Amazonia (Brazil) and implications for biogeography and evolution. *Quaternary Research*, *63*, 78—89.

Rozo, J. M. G., Nogueira, A. C. R., & Carvalho, A. S. (2005). Análise multitemporal do sistema fluvial do Amazonas entre a ilha do Careiro e a foz do rio Madeira. *Anais XII Simpósio Brasileiro de Sensoriamento Remoto* (pp. 1875—1882). Goiânia, Brazil.

Salo, J., Kalliola, R., Hakkinen, I., Makinen, Y., Niemela, P., Puhakka, M., et al. (1986). River dynamics and the diversity of the Amazon lowland forest. *Nature*, *322*, 254—258.

Schöngart, J. (2003). Dendrochronologische Untersuchungen in Überschwemmungswäldern der várzea Zentralamazoniens. In H. Böhnel, H. Tiessen, & H. J. Weidelt (Eds.), *Göttinger Beiträge zur Land- und Forstwirtschaft in den Tropen und Subtropen, Vol 149* (pp. 1—257). Göttingen, Germany.

Schöngart, J., Piedade, M. T. F., Wittmann, F., Junk, W. J., & Worbes, M. (2005). Wood growth patterns of *Macrolobium acaciifolium* (Benth.) Benth. (Fabaceae) in Amazonian black-water and white-water floodplain forests. *Oecologia*, *145*(3), 454—461.

Schöngart, J., & Junk, W. J. (2007). Forecasting the flood pulse in central Amazonia by ENSO-indices. *Journal of Hydrology*, *335*, 124—132.

Sioli, H. (1954). Beiträge zur regionalen Limnologie des Amazonasgebietes. *Archiv für Hydrobiologie*, *45*, 267—283.

Sioli, H. (1984). The Amazon and its main affluents: Hydrography, morphology of the river courses, and river types. In H. Sioli (Ed.), *The Amazon: Limnology and landscape ecology of a mighty tropical river and its basin* (pp. 127—166). Dordrecht: Dr W Junk Publishers.

Sociedade Civil Mamirauá — SCM, Conselho Nacional de Desenvolvimento Científico e Tecnológico-CNPq/MCT, Instituto de Proteção Ambiental do Estado do Amazonas-IPAAM (Eds.) (1996). *Mamirauá, Plano de Manejo (síntese)* (pp. 1–96). Brasília.

Sternberg, H. O. (1998). *A água e o homem na várzea do Careiro*, 2ª Edição Belém, Brazil: Museu Paraense Emílio Goeldi.

Wittmann, F., Anhuf, D., & Junk, W. J. (2002). Tree species distribution and community structure of central Amazonian várzea forests by remote-sensing techniques. *Journal of Tropical Ecology*, *18*, 805—820.

Wittmann, F., & Junk, W. J. (2003). Sapling communities in Amazonian white-water forests. *Journal of Biogeography*, *30*, 1533—1544.

Wittmann, F., Junk, W. J., & Piedade, M. T. F. (2004). The várzea forests in Amazonia: Flooding and the highly dynamic geomorphology interact with natural forest succession. *Forest Ecology and Management*, *196*, 199—212.

Wittmann, F., Schöngart, J., Montero, J. C., Motzer, T., Junk, W. J., Piedade, M. T. F., et al. (2006). Tree species composition and diversity gradients in white-water forests across the Amazon basin. *Journal of Biogeography*, *33*, 1334—1347.

Worbes, M., Klinge, H., Revilla, J. D., & Martius, C. (1992). On the dynamics, floristic subdivision and geographical distribution of várzea forests in Central Amazonia. *Journal of Vegetation Science*, *3*, 553—564.